Received: 5 December 2024 | Revised: 12 February 2025 | Accepted: 26 February 2025 | Published online: 24 March 2025

RESEARCH ARTICLE

Journal of Optics and Photonics Research
2025, Vol. 00(00) 1–7
DOI: 10.47852/bonviewJOPR52024969

BON VIEW PUBLISHING

Optical Antenna of Complex Molecule: Simulation of Anisotropic Global Dipole

Mufei Xiao[1,*], Hyrum Contreras-Jimenez[2], Jessica Méndez-Velarde[2], Roberto Núñez-González[3], Joel Antúnez-García[2], Fabian N. Murrieta-Rico[4], Constanza Koop-Santa[5], Armando Reyes-Serrato[1], Vitalii Petranovskii[1] and Nikifor Rakov[6]

[1]*Center for Nanosciences and Nanotechnology, National Autonomous University of Mexico, Mexico*

[2]*Faculty of Sciences, Autonomous University of Baja California, Mexico*

[3]*Department of Mathematics, University of Sonora, Mexico*

[4]*Mechatronics Engineering, Polytechnic University of Baja California, Mexico*

[5]*Tecnológico de Monterrey, School of Engineering and Sciences, Mexico*

[6]*IPCM-Materials Science, Federal University of Vale do São Francisco, Brazil*

Abstract: Work is reported on optical antennas of complex molecules. Optical antennas of a nanometric particle are widely considered for light relays in various on-chip applications. An appealing candidate for an optical antenna is a complex molecule, for example, a huge cell containing a few hundred atoms. The optical properties, such as the radiation patterns, of the antennas may be optimized. The optimization includes the design and synthesis of the contents and structures of the molecule, such as the participating atoms and their positions. A convenient method to simulate the antenna is to solve the local field at the sites of atoms, self-consistently. A revolutionary proposal is to treat the molecule as a single dipole. Therefore, the molecule can be treated as a dipole in further simulations, and the degree of the isotropic property becomes visualizable. An isotropic radiator has an angular dependence, and a global dipole is a collective radiator. In the present work, we show that by making use of the density function theory one can calculate the global band caps. Based on the calculated density of states distribution, one obtains various optical parameters of the global dipole, including the polarizability of the dipole. Our attention is concentrated on the degree of anisotropy of the dipole, as it modifies dramatically the radiation pattern of the antenna.

Keywords: optical antenna, light relay, complex molecule, DFT, anisotropic global dipole

1. Introduction

Silicon chips are more and more saturated and optical relays become plausible to speed up the transportation of signals and to avoid electric losses [1, 2]. There have been developed quite a lot of so-called optical antennas for the task of light relay on a chip [3, 4]. Among others, optical antennas have been designed with a single particle of metallic or semiconductor materials, metallic structures printed on the chip, as well as an ensemble or a chain of particles [5, 6]. It is worth introducing complex molecules for the role of optical antennas, as they may replace a group of particles [7]. Complex molecules may be chemically synthesized and some hundreds of different atoms are bound together as a molecule. Therefore, it becomes possible to construct optical antennas with desirable properties, such as the efficiency of light transportation and radiation pattern. The optical parameters of the complex molecules are determined by the contents and structures, that is, the member atoms and their positions. Metallic atoms play usually important roles. The structures and the distances between the atoms are essential for the global optical properties, as the interactions between the atoms may trigger resonant plasmons. The optical excitation and the radiation of the molecule depend on the local field at each molecule.

From both theoretical and numerical viewpoints, a convenient method for simulating an optical antenna that is composed of a group of point-like particles is to make use of the field propagator (Green's function) approach [7–15]. The simulation is divided into two steps, namely the particle reaction to the external excitation and the superposition of the radiation stemming from each particle. The Green's function approach has been widely used for optical simulations [8–15]. However, for simulating optical antennas, the approach can hardly establish relations between the radiation properties, such as strength and pattern, and the structure of the molecule antennas, such as the participating atoms and their positions. Therefore, the numerical simulation can hardly provide guides for the design and synthesis of the complex molecule. For these reasons, novel approaches are urgently needed to establish concise and visualizable relations between the antenna radiation

*Corresponding author: Mufei Xiao, Center for Nanosciences and Nanotechnology, National Autonomous University of Mexico, Mexico. Email: mufei@ens.cnyn.unam.mx

and the structure of the molecule, so that the design and the synthesis receive clear and direct guidance.

Using complex molecules is certainly attractive as it provides extra properties that a single antenna of metal and semiconductor cannot offer. However, it is complicated to assess the antenna properties of the complex molecule. To determine the antenna properties one has often to resort to experiments.

In the present work, we introduce a revolutionary approach for the simulation of complex molecules for optical antennas. There are also two steps. First, one carries out the density function theory (DFT) simulation of the whole molecule to obtain the global band caps. Based on the calculated density of states (DOS), one calculates key material and optical parameters of the molecule. In other words, we treat the molecule as a huge dipole [16–20]. The second step is to deal with the radiation of a single dipole [16]. Not only does the simulation of the dipole radiation become simple and direct but also it appears clear the dipole parameters. In this case, one knows what to do for optimization of the dipole. For example, the degree of isotropy of the dipole determines largely the radiation property of the antenna. In particular, the degree of isotropy is shown by the value of the off-axis elements of the global dipole. Since the dyadic response tensors, such as the polarizability and the dielectric function, of the global dipole are known from the first step, that is, the DFT simulation, the guidance for the design and synthesis becomes clear and direct. Of course, the simulation difficulties shift to the DFT calculations. Nowadays, it becomes possible to simulate complex molecules of a few hundred atoms with parallel supercomputers. We show in the present work, a few examples.

Note in passing that the above-proposed approach for simulating a group of bound particles is not limited to dealing with optical antennas using complex molecules. Similar thought would be useful for various applications where a tightly bound group of particles is involved, especially for near-field radiation within nanometric spacing. It would be interesting to have a systematic comparison between the field propagator (Green's function) approach and the global dipole approach that is introduced in the present paper, which will be in our forthcoming work. We stress that the term cell used in the present work is to describe a microscopic system that requires quantum mechanics to simulate their DOS distribution.

We organize the present paper as follows. In Section 2, the theory is presented and the numerical procedures are outlined for both Green's function and global dipole approaches, as well as the details of calculations for optical properties of the global dipole from the DOS distributions. In Section 3, numerical results are presented and discussed. Examples of Green's function approach are presented. DFT simulation of an LTA zeolite is presented. The influence of the isotropy of the global dipole is discussed. In Section 4, the work is concluded with the perspectives of the proposal.

2. Theory and Calculation

Within the present section, theoretical and numerical procedures are outlined both for Green's function approach and the so-called global dipole approach with detailed theoretical backgrounds as well as computational implementations.

First, the two steps of Green's function approach are presented for a group of nanometric particles. The particles are assumed optically active and tightly bound together within nanometric distances. The situation includes cells of many atoms. Note that, not all atoms in a complex molecule are optically active. There should be differences from the point of view of a global dipole. The less active atoms are useful components for the global reaction of the cell. Nevertheless, internal and between-particle interactions are taken into account. An exciting field modifies the local field at each particle. The process can be described with a self-consistent equation set as [8, 9]

$$\vec{E}(\vec{R}_i,\omega)=\vec{E}_0(\vec{R}_i,\omega)-\mu\omega^2\sum_{j=1}^{j=N}\overleftrightarrow{G}(\vec{R}_i,\vec{R}_j,\omega)\cdot\left[\overleftrightarrow{\alpha}_j(\omega)\cdot\vec{E}(\vec{R}_j,\omega)\right] \tag{1}$$

where $\vec{E}_0(\vec{R}_i,\omega)$ and $\vec{E}(\vec{R}_i,\omega)$ are respectively the monochromatic incident field and the local field of angular frequency at the particle site. The field propagator (or dyadic Green's function) in free space describes the field propagation from j particle to i particle,

$$\overleftrightarrow{G}(\vec{R}_i,\vec{R}_j,\omega)=\frac{1}{4\pi}\left[\left(-\frac{1}{R}-\frac{ic}{\omega R^2}+\frac{c^2}{\omega^2R^3}\right)\overleftrightarrow{U}+\left(\frac{1}{R}+\frac{3ic}{\omega R^2}-\frac{3c^2}{\omega^2R^3}\right)\vec{e}_R\vec{e}_R\right]\exp\left(i\vec{k}\cdot\vec{R}\right) \tag{2}$$

for the vector $\vec{R}=\vec{R}_j-\vec{R}_j$ and distance $R=\left|\vec{R}_j-\vec{R}_j\right|$, $\vec{e}_R=\left(\vec{R}_j-\vec{R}_i\right)/R$ is a unit vector, $\overleftrightarrow{U}$ is a unit tensor, and $k=\omega/c$ is the wavenumber. The polarizability tensor is calculated within the long wavelength approximation via the radius a and the dielectric function $\varepsilon(\omega)$ as

$$\overleftrightarrow{\alpha}(\omega)=4\pi\varepsilon_0a^3\frac{\varepsilon(\omega)-1}{\varepsilon(\omega)+2}\begin{pmatrix}1&0&0\\0&1&0\\0&0&1\end{pmatrix} \tag{3}$$

And, after the local field is determined by the proven self-consistent equation, the scattering field at an outside position $\vec{r}$ can then be calculated as

$$\vec{E}(\vec{r},\omega)=-\mu\omega^2\sum_{j=1}^{N}\overleftrightarrow{G}(\vec{r},\vec{R}_j,\omega)\cdot\left[\overleftrightarrow{\alpha}_j(\omega)\cdot\vec{E}(\vec{R}_j,\omega)\right] \tag{4}$$

Therefore, the scattered field at an outside distance with a specific direction is obtained as a superposition of the radiation from each emitter.

Equation (1) shows that the field at each particle stems from a sum of contributions of other particles with various polarizability of which the strength is shown in Equation (3). The interactions between particles are included in the field propagators in Equation (2). One solves the set of equations self-consistently as a standard eigenvalue problem. It is expected that the local field can be accurately calculated with possible resonances. Once the local field is obtained, the observed field at a point away from the cluster is calculated with the equation in Equation (4) which represents the optical response of the cluster. The details of the field propagators involved in the numerical simulations can also be found in references [8, 9]. Note in passing that, the lengths were normalized to the wavelength.

A key component in the above theory is the field propagators or Green's functions in Equation (2). For optical antenna in on-chip applications, suitable field propagators are available for near-field and evanescent fields. Considering the work environment of the optical antenna, a reflection field propagator may be useful. An evanescent field propagator suitable for near-field distances is as follows:

$$\overleftrightarrow{G}_{evan}(\vec{R}_i,\vec{R}_j,\omega) = \frac{1}{4\pi}\left[\left(-\frac{1}{2R}+\frac{c^2}{\omega^2}\frac{1}{R^3}\right)\overleftrightarrow{U}+\left(-\frac{1}{2R}-\frac{3c^2}{\omega^2}\frac{1}{R^3}\right)\vec{e}_R\vec{e}_R\right]\exp\left(i\vec{k}\cdot\vec{R}\right) \tag{5}$$

The indirect evanescent and propagating field propagators are more complicated. It is essential for dealing with reflection within nanometric surfaces. The readers are referred to References [8, 9] for more details. In the numerical section, some examples are presented using the above formalism to show the usefulness of the theory for optical-antenna-related simulations.

Second, we outline the global dipole approach. The calculations of the electronic structure are fulfilled with the full potential linearized augment plane wave method The LAPW method is an implementation of the Kohn-Sham version of the widely used DFT. It deals with both valence and core electrons on the same footing in the context of DFT. We use the platform of the WIEN2K program [21–23]. It makes use of the random phase approximation for the boundaries as well as the generalized gradient approximation for the potentials. The set of eigen equations for a many-electron system is shown below:

$$\left(-\frac{\hbar^2}{2m}\nabla^2+v_{eff}(\vec{R})\right)\phi_i(\vec{R}) = \varepsilon_i\varphi_i(\vec{R}) \tag{6}$$

which is indeed the Kohn–Sham equation. In the equation, the potential $v_{eff}(\vec{r})$ is called the Kohn-Sham potential. ε_i is the eigenenergy. The wave function $\phi_i(\vec{r})$ which is spin degenerated is referred to as the Kohn-Sham orbital energy. For an N electron system, the total electron density can be written as a sum of individual Kohn-Sham orbital densities as

$$\rho(\vec{R}) = \sum_{i=1}^{i=N}\left|\phi_i(\vec{R})\right|^2 \tag{7}$$

and the total energy of the system becomes

$$\begin{aligned} E(\rho) = {} & \int v_{ext}(\vec{R})\rho(\vec{R})d\vec{R}+ \\ & \sum_{i=1}^{N}\int\phi_i^*(\vec{R})\left(-\tfrac{\hbar^2}{2m}\nabla^2\right)\phi_i(\vec{R})d\vec{R}+ \\ & e^2\iint\frac{\rho(\vec{R})\rho(\vec{R}')}{\left|\vec{R}-\vec{R}'\right|}d\vec{R}d\vec{R}'+E_{xc}(\rho) \end{aligned} \tag{8}$$

where the first term denotes the Joule energy, the second term refers to the kinetic energy, the third term is the so-called Hartree energy, and the last term represents the exchange-correlation energy. The effective Kohn-Sham potential is to be obtained from a derivation of the total energy, as

$$\begin{aligned} v_{eff}(\rho) &= v_{ext}(\vec{R})+e^2\int\frac{\rho(\vec{R}')}{\left|\vec{R}-\vec{R}'\right|}d\vec{R}'+\frac{\partial E_{xc}(\rho)}{\partial\rho} \\ &\equiv v_{ext}(\vec{R})+v_H(\vec{R})+v_{xc}(\vec{R}) \end{aligned} \tag{9}$$

where the second term is the Hartree potential and the last term represents the exchange-correlation potential. A self-consistent iterative procedure is implemented to calculate the Kohn-Sham potential from an initial electron density. With a solution of Equation (6) and the relation in Equation (8), one obtains a new electron density. The process goes on till the initial and new densities are identical, which means that the ground state density has been found, as the energy is the lowest.

When the electronic structure is known, various optical parameters are to be extracted from possible interband transitions. Optical calculations are performed in the random phase. The dielectric function is obtained by calculating matrix elements between the occupied and unoccupied states [24]:

$$\mathrm{Im}\left\{\varepsilon_{\alpha\beta}(\omega)\right\} = \frac{\hbar^2e^2}{\pi m^2\omega^2}\sum_n\int dk\left\langle\psi_k^{C_n}\middle|P^\alpha\middle|\psi_k^{V_n}\right\rangle\left\langle\psi_k^{V_n}\middle|P^\beta\middle|\psi_k^{C_n}\right\rangle\delta\left(E_k^{C_n}-E_k^{V_n}-\omega\right) \tag{10}$$

where the matrix elements are obtained. The real part was obtained by the widely used Kramers-Kronig transformation:

$$\mathrm{Re}\left\{\varepsilon_{\alpha\beta}(\omega)\right\} = \delta_{\alpha\beta}+\frac{2}{\pi}P\int_0^\infty\frac{\omega'\mathrm{Im}\,\varepsilon_{\alpha\beta}(\omega')}{(\omega')^2-\omega^2} \tag{11}$$

The reflectivity at normal incidence can be calculated by:

$$R_{\alpha\beta}(\omega) = \frac{[n(\omega)-1]^2+\kappa^2(\omega)}{[n(\omega)+1]^2+\kappa^2(\omega)} \tag{12}$$

In Equation (12), n and κ are real and imaginary refractive index, also as refractive index and the extinction coefficient, respectively. The refractive index and the extinction coefficient can be conveniently extracted from the following relations:

$$n_{\alpha\beta}(\omega) = \frac{1}{2}\left|\varepsilon_{\alpha\beta}(\omega)+\mathrm{Re}\left\{\varepsilon_{\alpha\beta}(\omega)\right\}\right|^{1/2} \tag{13}$$

$$\kappa_{\alpha\beta}(\omega) = \frac{1}{2}\left|\varepsilon_{\alpha\beta}(\omega)-\mathrm{Re}\left\{\varepsilon_{\alpha\beta}(\omega)\right\}\right|^{1/2} \tag{14}$$

The absorption coefficient and the optical conductivity can also be calculated.

$$\alpha_{\alpha\beta}(\omega) = \frac{2\omega\kappa_{\alpha\beta}(\omega)}{c} \tag{15}$$

$$\sigma_{\alpha\beta}(\omega) = \frac{\omega}{4\pi}\mathrm{Im}\left\{\varepsilon_{\alpha\beta}(\omega)\right\} \tag{16}$$

The electron energy loss function is given by

$$L_{\alpha\beta}(\omega) = -\mathrm{Im}\left\{\frac{1}{\varepsilon_{\alpha\beta}(\omega)}\right\} \tag{17}$$

The above quantities are 3×3 tensors and their elements determine the properties of the global dipole. The radiation strength and pattern can be modified when some of the elements are changed. Therefore, it becomes possible to simulate complex molecules to obtain specific antenna radiation, such as the anisotropy of the dipole.

It is expected that the optical properties are anisotropic for the clusters, which implies that all the functions are 3×3 tensors with non-zero off-diagonal elements. Since the tensors are symmetric, the theoretical process should be able to output 6 elements, i.e., 3 diagonal elements and 3 off-diagonal elements. The 6 elements are schematically shown in Equation (18) with a 3×3 tensor $\overleftrightarrow{a}$, with 3 diagonal elements a_{xx}, a_{yy}, and a_{zz}, and 3 off-diagonal elements (the other 3 elements are symmetric) $a_{xy}=a_{yx}$, $a_{xz}=a_{xy}$, and $a_{xz}=a_{xx}$.

$$\overleftrightarrow{a} = \begin{pmatrix} a_{xx} & a_{xy} & a_{xz} \\ a_{yx} & a_{yy} & a_{yz} \\ a_{zx} & a_{zy} & a_{zz} \end{pmatrix} \tag{18}$$

In the following numerical section, we show the dependence of the degree of the isotropy of the global dipole on some tensor elements.

3. Results and Discussions

Numerical results are presented in the present section based on the formalism presented in the previous section. Numerical results are included from both the field propagator approach and the global dipole approach. The examples presented for the field propagator approach are intended to demonstrate the usefulness of the simulation for nanometric and on-chip environments, as well as the shortbacks and limitations of the method for assessing the optical antenna pattern, and the need for the proposed global dipole approach.

We start with a simple example, a silver sphere placed on a silver substrate. We consider only the distances within the near-field range as it would be the environment where the on-chip optical antenna is suggested to work. A 30 nm probe sphere scans over the object sphere for various polarization configurations. These images reflect mainly the symmetry properties of the near-field components of a dipole field.

Note that the dipole radiation patterns are rich and controlled by the incident field. Therefore, the method is useful for studying single-particle radiation in nanometric environments. In addition to Figure 1, we show that it may also be useful for a group of particles. In Figure 2, it shows an example.

Figure 2 demonstrates an application of the field propagator for a group of particles. Note that the near field becomes complicated and depends on the polarization of the incident field. The particles are placed to form an arrow. Both Figures 1 and 2 show the usefulness of the field propagator (Green's function) simulations for nanometric scale applications. However, there are drawbacks and limitations. For more examples, one is referred to References [8, 9, 15]. The present work is to introduce the global dipole approach.

For complex molecules, it is reasonable to have a global dipole, that is, the whole group emitters are considered as a single dipole. A single dipole is easy to handle and radiation patterns especially the directions are related to the tenor elements of the polarizability. For example, the degree of anisotropy is related to the off-axis elements. Therefore, the simulation task shifts to calculate the giant cell of many atoms. Using DFT, one can calculate the DOS distribution of molecules with a few hundred atoms. The optical inactive atoms are usually neglected in Green's function approach, while all atoms are meaningful within the global dipole approach.

An example of global dipole simulation is shown as follows. We choose an LTA zeolite as the complex molecule. Zeolite is a mesoscopic porous catalysis. The structure of the cell is schematically shown in Figure 3(a) with the calculated DOS map in Figure 3(b). There are about 168 atoms of various kinds in the cell.

With the DOS map in Figure 4, one can calculate most of the material and optical parameters. The parameters and the corresponding formalism to calculate them are listed in the previous section of the theory. Figure 4 shows the reflectivity plot, which is relevant to the present work. There are various simple methods to estimate the dipole polarizability from the reflectance, or directly use the reflectance for scattering. An alternative is to estimate the polarizability using Rayleigh's formula in Equation (3). As far as the radiation pattern is concerned, one can use directly the reflectance tensor. The tensor elements shown in Figure 4 include three on-axis elements and three off-axis elements, and the tensors are symmetric.

It is interesting to see in Figure 4 that the off-axis elements are significant and strong, which implies strong anisotropic behaviors.

Figure 1
Near-field images of the field components (a) horizontal; (b) circular right-hand; (c) vertical; (d) circular left-hand, at the site of a 30 nm glass probe sphere, which is scanned in a constant-height plane (71 nm away from the surface) over a 20 nm silver sphere placed on a silver substrate, for the incident field polarized linearly (a, c) in the horizontal direction and right-hand circularly (b, d). The grayscale bar unit is arbitrary

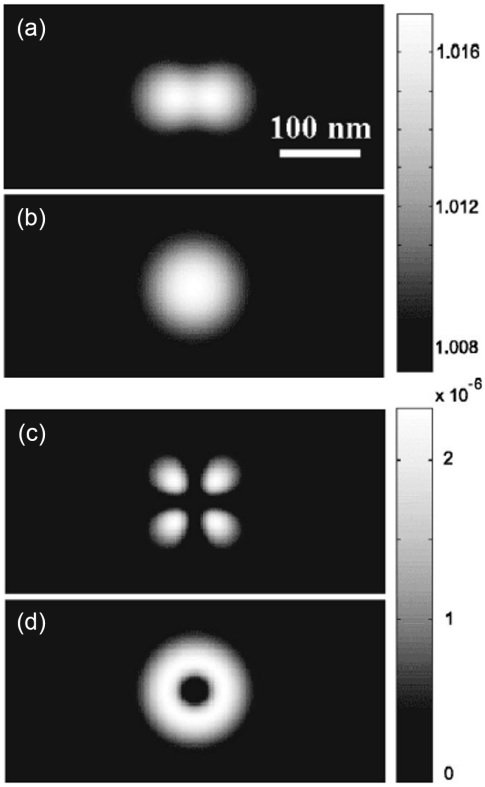

Figure 2
Near-field images of the circular right-hand component of the self-consistent field at the site of 43 silver spheres of 20 nm. The incident light is a right-hand circularly polarized unit field. The grayscale bar unit is arbitrary

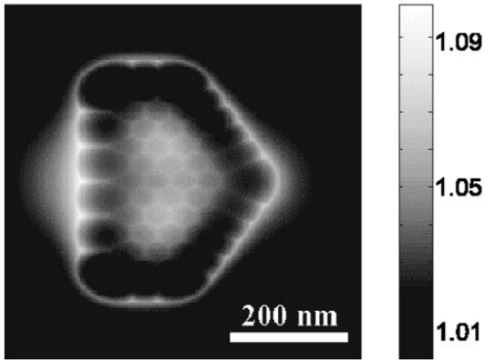

Figure 3
(a) The optimized unit cell of zeolite LTA with a triclinic structure, red, blue, dark blue, and yellow spheres corresponds to O, Al, Si, and Na atoms, respectively, (b) The calculated band structure

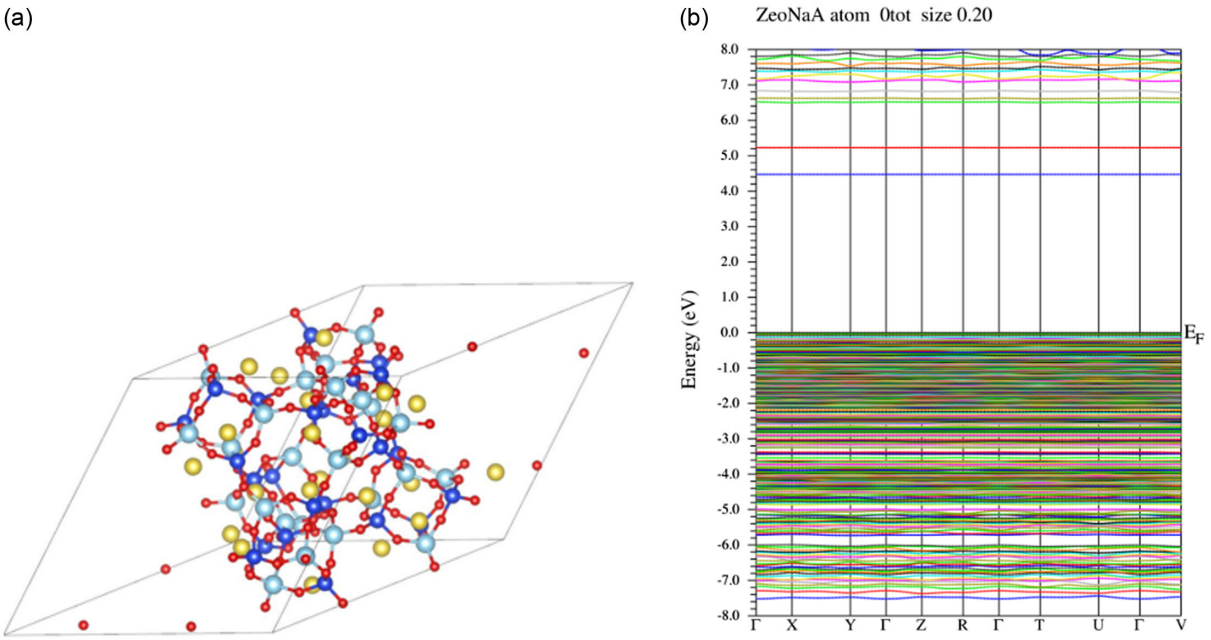

Figure 4
Spectral of 6 tensor elements of the reflectivity

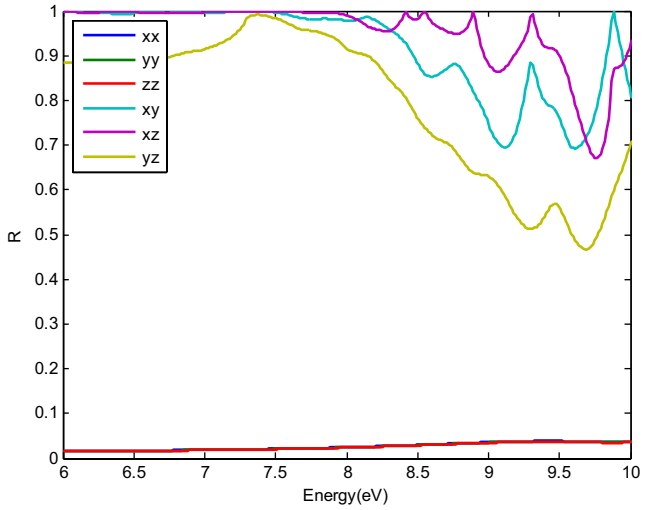

Figure 5
Contour and image distributions of dipolar radiations with a vertical incident field, (a) a dipole, and (b) a zeolite with anisotropic optical response. The range is about r < 12 nm for 5 eV light, or 249 nm in wavelength. The incident light is polarized in the z-axis toward the paper

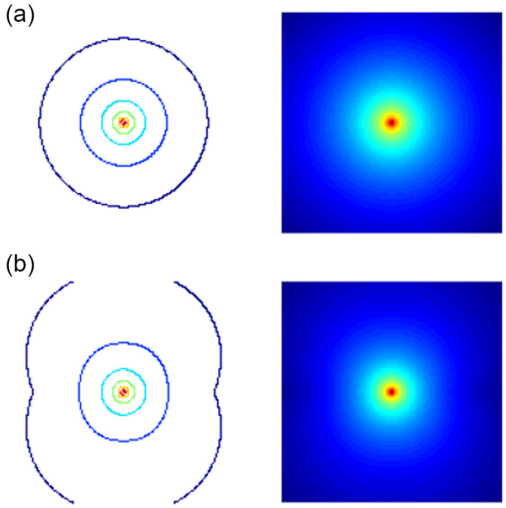

If the off-axis elements are absent, the dipole is highly isotropic, and the dipole radiation follows the simple dipoles, whereas if the off-axis elements are significant, the dipole is anisotropic. Anisotropic dipoles radiate in specific directions. Optical antenna designs look for oriented dipoles so that light is concentrated in a direction. For the present example, the active spectrum falls in ultraviolet and varies with the light frequency. Of course, there are many molecules suitable for other frequency ranges, and the variation in the spectrum would provide an opportunity to externally control the dipole radiation.

In terminating, we present a comparison of the radiation patterns. In Figure 5(a), the radiation pattern of a textbook dipole is presented [25], which is isotropic for the vertical incident field. In Figure 5(b), the radiation pattern of the zeolite is shown in Figure 5(b), which appears anisotropic with a specific direction. Further studies are needed to look for suitable molecules for optical antennas. By modifying the structure of the molecules, one can control the degree of anisotropy of the global dipole. The present work is mainly to propose the global dipole approach. The revolutionary approach would bring about novel applications as a

useful simulation tool. The novel approach does not expel the Green's function approach. Both approaches are useful for dealing with optics in nanometric environments. However, the proposed global dipole approach appears more suitable for studying optical antennas of complex molecules.

4. Conclusion and Perspective

In conclusion, a novel approach is proposed for the design of optical antennas of complex molecules. Optical antennas are widely considered for light relay in various on-chip applications. An appealing candidate for an optical antenna is a complex molecule, for example, a huge cell containing a few hundred atoms. The optical properties, such as the radiation patterns, of the antennas may be optimized. The optimization includes the design and synthesis of the contents and structures of the molecule, such as the participating atoms and their positions. A convenient method to simulate the antenna is to solve the local field at the sites of atoms, self-consistently. We have in the present work proposed a novel method to treat the molecule as a single dipole. Therefore, the degree of the isotropic property becomes visualizable. In the present work, we have shown that by making use of the DFT one can calculate the global band caps. Here, the global band caps are from calculations of the whole system. Based on the DOS one obtains various optical parameters of the global dipole, including the polarizability of the dipole. Our attention is concentrated on the degree of anisotropy of the dipole, as it modifies dramatically the radiation distribution of the antenna. The thought of a global dipole approach will be useful for other applications, where scatters are complex molecules contained in a nanometric geometry. Detection of light in such spaces is still a challenge and unreliable. Considering the huge cells as a single global dipole may guide the design and synthesis of the molecules. Overall we believe that the proposed global dipole approach would find a wide range of applications, such as on-chip light sourcing and waveguiding. The proposal is unique and novel within the literature about optical antennas.

Note in terminating that although the proposed global dipole approach is primarily intended for dealing with optical dipole interactions within the near-field range, there is no restriction to extending to the middle and far field ranges [26, 27].

Acknowledgements

R.N.G. is grateful to ACARUS at Universidad de Sonora for the computer time support.

Funding Support

This research is funded by DGAPA-PAPIIT Grant IG101623.

Ethical Statement

This study does not contain any studies with human or animal subjects performed by any of the authors.

Conflicts of Interest

The authors declare that they have no conflicts of interest to this work.

Data Availability Statement

Data sharing is not applicable to this article as no new data were created or analyzed in this study.

Author Contribution Statement

Mufei Xiao: Conceptualization, Methodology, Software, Formal analysis, Investigation, Resources, Data curation, Writing – original draft, Writing – review & editing, Visualization, Supervision, Project administration, Funding acquisition. **Hyrum Contreras-Jimenez:** Data curation, Writing – original draft, Writing – review & editing, Visualization, Funding acquisition. **Jessica Méndez-Velarde:** Data curation, Writing – original draft, Writing – review & editing, Visualization, Funding acquisition. **Roberto Núñez-González:** Validation, Data curation, Writing – original draft, Writing – review & editing, Visualization, Funding acquisition. **Joel Antúnez-García:** Validation, Data curation, Writing – original draft, Writing – review & editing, Visualization, Funding acquisition. **Fabian N. Murrieta-Rico:** Data curation, Writing – original draft, Writing – review & editing, Visualization, Funding acquisition. **Constanza Koop-Santa:** Data curation, Writing – original draft, Writing – review & editing, Visualization, Funding acquisition. **Armando Reyes-Serrato:** Data curation, Writing – original draft, Writing – review & editing, Visualization, Funding acquisition. **Vitalii Petranovskii:** Data curation, Writing – original draft, Writing – review & editing, Visualization, Funding acquisition. **Nikifor Rakov:** Data curation, Writing – original draft, Writing – review & editing, Visualization, Funding acquisition.

References

[1] Novotny, L., & Van Hulst, N. (2011). Antennas for light. *Nature Photonics*, *5*(2), 83–90.

[2] Moazen Dehkordi, S., & Mohammadi, H. (2024). Improvement of directivity in plasmonic nanoantennas based on structured cubic gold nanoparticles. *Scientific Reports*, *14*(1), 17153. https://doi.org/10.1038/s41598-024-68320-y

[3] Habib, A., Zhu, X., Fong, S., & Yanik, A. A. (2020). Active plasmonic nanoantenna: An emerging toolbox from photonics to neuroscience. *Nanophotonics*, *9*(12), 3805–3829. https://doi.org/10.1515/nanoph-2020-0275

[4] Kuen, L., Löffler, L., Tsarapkin, A., Zschiedrich, L., Feichtner, T., Burger, S., & Höflich, K. (2024). Chiral and directional optical emission from a dipole source coupled to a helical plasmonic antenna. *Applied Physics Letters*, *124*(23), 231102. https://doi.org/10.1063/5.0201748

[5] Li, Y., Li, Q., Lin, D., Feng, J., & Guo, J. (2024). Technologies and challenges of large-scale silicon photonic integrated circuit (Invited). *Acta Optica*, *44*, 1513015.

[6] Ji, C. L., Chen, H., Gao, Q., Han, J., Li, W., & Xie, J. (2024). Dinuclear gold-catalyzed divergent dechlorinative radical borylation of gem-dichloroalkanes. *Nature Communications*, *15*(1), 3721. https://doi.org/10.1038/s41467-024-48085-8

[7] Virmani, D., Maciel-Escudero, C., Hillenbrand, R., & Schnell, M. (2024). Experimental verification of field-enhanced molecular vibrational scattering at single infrared antennas. *Nature Communications*, *15*(1), 6760. https://doi.org/10.1038/s41467-024-50869-x

[8] Xiao, M. (1997). Theoretical treatment for scattering scanning near-field optical microscopy. *Journal of the Optical Society of America A*, *14*(11), 2977–2984. https://doi.org/10.1364/JOSAA.14.002977

[9] Xiao, M., Zayats, A., & Siqueiros, J. (1997). Scattering of surface-plasmon polaritons by dipoles near a surface: Optical near-field localization. *Physical Review B*, *55*(3), 1824. https://doi.org/10.1103/PhysRevB.55.1824

[10] Richard, N. (2000). Light scattering by supported metallic nanostructures: Polarization and spectroscopy in the near-field zone. *physica status solidi (b)*, *220*(2), 1009–1024. https://doi.org/10.1002/(SICI)1521-3951(200008)220:2<1009::AID-PSSB1009>3.0.CO;2-M

[11] Ben-Abdallah, P. (2024). Control of the local photonic density of states above magneto-optical metamaterials. *Physical Review B*, *109*(24), 245409. https://doi.org/10.1103/PhysRevB.109.245409

[12] Alebrahim, M. A., Ahmad, A. A., Migdadi, A. B., & Al-Bataineh, Q. M. (2024). Localize surface plasmon resonance of gold nanoparticles and their effect on the polyethylene oxide nanocomposite films. *Physica B: Condensed Matter*, *679*, 415805. https://doi.org/10.1016/j.physb.2024.415805

[13] Alzoubi, F. Y., Ahmad, A. A., Aljarrah, I. A., Migdadi, A. B., & Al-Bataineh, Q. M. (2023). Localize surface plasmon resonance of silver nanoparticles using Mie theory. *Journal of Materials Science: Materials in Electronics*, *34*(32), 2128. https://doi.org/10.1007/s10854-023-11304-x

[14] Ustimenko, N. A., Kornovan, D. F., Baryshnikova, K. V., Evlyukhin, A. B., & Petrov, M. I. (2022). Multipole Born series approach to light scattering by Mie-resonant nanoparticle structures. *Journal of Optics*, *24*(3), 035603. https://doi.org/10.1088/2040-8986/ac4a21

[15] Summueang, C., Pon-On, W., Supadee, L., & Boonchui, S. (2022). Electromagnetic description of the interaction between talcum and the rough surface of a composite material. *Journal of Electrostatics*, *115*, 103639. https://doi.org/10.1016/j.elstat.2021.103639

[16] Núñez-González, R., Xiao, M., Antúnez-García, J., Ponce-Ruiz, J. L., Reyes-Serrato, A., Petranovskii, V., . . . , & Rakov, N. (2023). First-principles study of optical properties of linde-type A zeolite. *physica status solidi (b)*, *260*(12), 2300378. https://doi.org/10.1002/pssb.202300378

[17] Chen, Y., Liu, G., Wei, L., Zhao, J., & Zhang, G. (2024). Effect of bending deformation on the electronic and optical properties of O atoms adsorbed by Be_3N_2. *Journal of Molecular Modeling*, *30*(5), 129. https://doi.org/10.1007/s00894-024-05924-1

[18] Chen, Y., Liu, G., Wei, L., He, J., & Zhang, G. (2023). Effects of tensile deformation on the electronic and optical properties of O atom adsorbed monolayer β-Be_3N_2. *Modern Physics Letters B*, *37*(26), 2350109. https://doi.org/10.1142/S0217984923501099

[19] Ullah, M., Ali, R., Murtaza, G., & Chen, Y. (2019). First principles investigation of Be_3X_2 (X = N, P, As) and their alloys for solar cell applications. *Journal of Alloys and Compounds*, *795*, 385–390. https://doi.org/10.1016/j.jallcom.2019.05.017

[20] Ullah, M., Murtaza, G., & Laref, A. (2019). Comprehensive study of the physical properties of Ba_3Pn_2 (Pn = N, P, As, Sb and Bi) through first principles technique. *Materials Research Express*, *6*(9), 095902. https://doi.org/10.1088/2053-1591/ab2c9a

[21] Blaha, P., Schwarz, K., Medsen, G. K. H., Kvasnicka, D., & Luitz, J. (2001). *WIEN2k, An Augmented Plane Wave Plus Local Orbitals Program for Calculating Crystal Properties*, Vienna, Austria: Vienna University Technology.

[22] Kolobov, V. I. (2003). Fokker–Planck modeling of electron kinetics in plasmas and semiconductors. *Computational Materials Science*, *28*(2), 302–320. https://doi.org/10.1016/S0927-0256(03)00115-0

[23] Abdullah, D., & Gupta, D. C. (2024). Analyzing the structural, optoelectronic, and thermoelectric properties of $InGeX_3$ (X = Br) perovskites via DFT computations. *Scientific Reports*, *14*(1), 23575. https://doi.org/10.1038/s41598-024-72745-w

[24] Wooten, F. (1972). *Optical properties of solids*. New York: Academic Press.

[25] Jackson, J. D. (2021). *Classical electrodynamics*. New York: John Wiley & Sons.

[26] Xi, M., Liu, C., Li, N., Zhang, S., & Wang, Z. (2022). Parallel aligned dipole–multipole plasmonic hybridization. *The Journal of Physical Chemistry C*, *126*(10), 4984–4994. https://doi.org/10.1021/acs.jpcc.2c00150

[27] Harris, N., Arnold, M. D., Blaber, M. G., & Ford, M. J. (2009). Plasmonic resonances of closely coupled gold nanosphere chains. *The Journal of Physical Chemistry C*, *113*(7), 2784–2791. https://doi.org/10.1021/jp8083869

How to Cite: Xiao, M., Contreras-Jimenez, H., Méndez-Velarde, J., Núñez-González, R., Antúnez-García, J., Murrieta-Rico, F. N., . . . , & Rakov, N. (2025). Optical Antenna of Complex Molecule: Simulation of Anisotropic Global Dipole. *Journal of Optics and Photonics Research*. https://doi.org/10.47852/bonviewJOPR52024969